Journal of Interdisciplinary Mathematics
ISSN: 0972-0502 (Print), ISSN: 2169-012X (Online)
Vol. 29 (2026), No. 3, pp. 681–692
DOI : 10.47974/JIM-2503

Derivation of theta-angle and geometric transformation for skew correction using homography matrix

Divya Sharma †
Shilpa Sharma *
Vaibhav Bhatnagar §
Department of Computer Applications
Manipal University Jaipur
Jaipur 303007
Rajasthan
India

Abstract

Detecting tilted and skewed vehicle license plates is a significant challenge, often leading to reduced detection accuracy. Traditional detection models struggle with such variations, affecting the efficiency of automated license plate monitoring systems. This research devised a novel skewed license plate detection model that effectively addresses the issue of tilted and skewed license plates. The proposed model calculates the four coordinates and the centroid coordinates of each plate. To differentiate the angular distortion of the tilted plates, the inverse of theta is calculated to convert the slope into an angle. Based on estimated angles the license plates are categorized as straight horizontal ($\theta \approx 0°$), clockwise skewed ($\theta > 0°$) and anticlockwise skewed ($\theta < 0°$). The tilted coordinates then transform the quadrilateral plate into a rectangular shape using the homography matrix. Applied to a dataset of 1100 vehicle images with varied skewed and complex weather conditioned images, the model demonstrates enhanced feature extraction and localization precision. Experimental results show 99% detection accuracy, with notable gains in precision, recall, and mAP, outperforming existing methods. The proposed model supports SDG 11: Sustainable Cities and Communities through enhanced intelligent traffic systems.

Subject Classification: *94A08.*

Keywords: *Homography matrix, Tilted, Rotation matrix, Affine transformation, Perspective transformation.*

---

† *E-mail:* **divya.sharma@jaipur.manipal.edu**
* *E-mail:* **shilpa.sharma@jaipur.manipal.edu (Corresponding Author)**
§ *E-mail:* **vaibhav.bhatnagar@jaipur.manipal.edu**

1. Introduction

Detecting vehicles and recognizing their license plate characters are one of the essential approaches in modern surveillance, traffic management, and security systems. The ALPR systems, i.e. Automatic License Plate Recognition system, contribute significantly to the advancement of traditional traffic management approaches [1]. Moreover, in security systems, ALPR improves access control, by confirming the entry only for the authorized vehicles, thereby enhancing safety protocols. Several significant challenges that can reduce the effectiveness of ALPR systems include the tilted and skewed license plates capture, motion blur, environmental factors, low image resolution, etc. [2]. To resolve these challenges, advanced image processing techniques are required to accommodate a wide range of image conditions. Tilted or skewed license plates are one of the significant challenges for the ALPR system, due to variation in camera positioning. License plates can be tilted horizontally or vertically, with angles ranging from 0° to 180° horizontally and 35° to 125° vertically [3]. The variation in license plate view complicates the process of license plate detection. As the standard license plate detection systems are trained to detect the straight license plates only. The tilted and skewed license plates make the characters nonaligned and difficult for the character recognition system to recognize the characters accurately. An effective and intelligent approach must be devised to address the issue of tilted license plate detection. YOLO models have reformed real-time object detection by combining speed and accuracy through their single-stage, grid-based architecture [4]. YOLO models process entire images in one pass using deep Convolutional Neural Networks (CNNs), enabling efficient detection of objects like license plates. The basic YOLO versions can efficiently detect the straight license plates but detecting tilted or skewed license plates are still an issue to be resolved. YOLOv7 stands out well when comparing different license plate detection models because of its significant accuracy, speed, and versatility balance [5]. Due to their consistent high precision rates of approx. 0.769, recall rates of 0.8571, and F1 scores of above 0.66. Even though more recent models provide better metrics, they frequently have higher processing requirements and might not be appropriate for all deployment situations [6].Mathematically, the ALPR problem can be formulated as a compound optimization task involving object detection and optical character recognition, where the goal is to minimize the error functions associated with both localization and recognition under varied real-world constraints by using equation eq.1:

$$\min_{\theta_d,\theta_r}\left(\mathcal{L}_{detect}\big(D_{\theta d}(I)\big)+\mathcal{L}_{recognize}\big(R_{\theta r}\big(D_{\theta d}(I)\big)\big)\right) \qquad Eq.1$$

Where, I denote the input image, θ_d and θ_r are the parameters of the detection and recognition models, respectively.

To address these geometric inconsistencies, proposed an enhanced version of detection model, integrating spatial transformation by learning anchor boxes aligned with skewed aspect ratios and projective warps. The model explicitly estimates both the centroid $C(x_c, y_c)$ and the four corner points $\{P_i(x_i, y_i)\}_{i=1}^{4}$ of each detected license plate. The corner coordinates are used to compute a homography matrix $H \in \mathbb{R}^{3*3}$, facilitating the transformation of an irregular quadrilateral into a canonical axis-aligned rectangular region. To calculate the accuracy measures, following evaluating metrics are calculated: precision P, recall R, and F1 score using equation eq.2 [7]

$$P = \frac{TP}{TP+FP}, R = \frac{TP}{TP+FN}, F1 = \frac{2PR}{P+R} \qquad Eq.2$$

Here, TP, FP, and FN represent the true positives, false positives, and false negatives values. Contributions of this work are summarized as:

- Formulation of tilt condition-based detection pipeline with affine-invariant transformation for skewed plate detection.
- Integration of homography estimation for geometric rectification of detected plates.
- Empirical evaluation on a real-world dataset exhibiting skew, complex weather, and low-resolution properties.

The paper is structured as follows. The core concepts and fundamentals of the traditional detection models are explained in Section 2. Section 3 provides the methodology and implementation details of the proposed detection model. The results of the proposed model are evaluated in section 4. Section 5 discusses the conclusion and the future work of the proposed work.

2. Related Work

Traditional license plate detection methods relied on image processing techniques such as grayscale conversion, adaptive thresholding, and contour analysis to isolate plates from vehicle images [8]. These methods primarily relied on classical computer vision techniques such as edge detection, color-based methods, and contour analysis [9]. In 2014, significant advancements were made in ALPR systems, focusing on enhancing detection accuracy and computational efficiency. The study provided a comprehensive review of various license plate localization techniques, analyzing their merits, limitations, computational requirements, detection success rates, and overall system accuracy [10]. The author [11] continued to evolve license plate detection and recognition, focusing on enhancing accuracy and computational efficiency. Authors proposed a system that converts color images to grayscale, applies adaptive thresholding, and utilizes vertical edge detection with the Sobel operator. Their method achieved a detection accuracy of 96.9% across 60 images. Similarly, the author in [12] developed a framework combining deep neural networks with Generative Adversarial Networks (GANs) for license plate detection and recognition. Their method employed a cascaded CNN for initial detection, followed by a sequence labeling approach using Recurrent Neural

Networks (RNNs) for character recognition. The integration of GANs facilitated the generation of synthetic training data, thereby improving the robustness and accuracy of the recognition system. Researchers developed an automated license plate detection and recognition system combining wavelet decomposition and CNNs. The system detects license plates by extracting vertical edges using two-dimensional wavelet transforms and employs a CNN classifier for verification. Subsequent character segmentation and recognition are performed using another CNN, achieving high accuracy rates in both detection and recognition tasks [13].

2.1 *YOLO: Mathematical Foundation and Evolution*

The YOLO (You Only Look Once) family of object detection models is grounded in the principle of formulating object localization and classification as a single unified regression problem over spatially divided image grid [14]. Given an input image $I \epsilon \mathbb{R}^{H*W*C}$, the objective is to compute a set of bounding boxes $\{(x_i, y_i, w_i, h_i, c_i)\}$ where (x_i, y_i) represent the center coordinates, (w_i, h_i) the width and height, and $c_i \epsilon \mathbb{R}^K$ the class confidence scores over K classes [15].

YOLOv1: Unified Detection

YOLOv1 reformulated detection as a regression task. The image is partitioned into S×S grid, and each cell predicts bounding boxes, Each with 5 parameters: (x,y,w,h,conf), C class probabilities [1]. The loss function $\mathcal{L}YOLO_{v1}$ combines localization, confidence, and classification losses as in equation eq.3.

$$\mathcal{L} = \lambda_{coord} \sum_{i=1}^{S^2} \sum_{j=1}^{B} 1_{ij}^{obj} \left[(x-\hat{x})^2 + (y-\hat{y})^2 + (w-\hat{w})^2 ((h-\hat{h})^2) \right] + \dots \qquad Eq.3$$

YOLOv2: Anchor Box Formulation

YOLOv2 incorporated anchor boxes A = $\{a_k\}\ _k^K = 1 \epsilon \mathbb{R}^2$ for better bounding box priors, aligning the model closer to region proposal-based detectors [16]. Multi-scale training allowed model adaptation and the loss function revised to be anchor-sensitive using equation eq.4.

$$\mathcal{L}YOLO_{v2} = \sum_{i,k} 1_{ik}^{obj}. Smooth_{l1}(regression\ error) + Classification\ loss. \qquad Eq.4$$

YOLOv3: Feature Pyramid Networks (FPN)

YOLOv3 extended the architecture with Feature Pyramid Networks, it used binary cross-entropy loss for class prediction instead of softmax, enabling multilabel classification as equation eq.5 [17].

$$\mathcal{L}_{Class} = -\sum_c y_c \log \widehat{Pc} + (1-y_c) \log\left(1-\hat{P}_c\right) \qquad Eq.5$$

YOLOv4: Optimized Backbone and Activation

YOLOv4 introduced CSPDarknet53 as the backbone, integrated the Mish activation using equation eq.6. and adopted IoU loss for bounding box regression using equation eq.7 [18].

$$Mish(x) = x.\tanh\left(In(1 + e^{x})\right) \qquad Eq.6$$

$$\mathcal{L}_{CIOU} = 1 - IOU + \frac{\rho^2(b,b^{gt})}{C^2} + av \qquad Eq.7$$

where ρ is the Euclidean distance between box centers, and v encodes aspect ratio consistency.

YOLOv5: Lightweight Deployment

YOLOv5, though unofficial, gained attention due to its modular PyTorch implementation and deployment flexibility [19] [20]. It included an auto-learning bounding box anchor mechanism and utilized scaled cosine learning rate schedules to optimize convergence.

YOLOv6: Industrial Orientation

YOLOv6 was developed with industrial applications in mind, optimizing computational complexity while retaining detection fidelity [21]. It incorporated efficient block reuse and knowledge distillation for real-time applications on edge devices.

YOLOv7: Mathematical Innovations and Suitability for License Plate Detection

YOLOv7 introduced Extended Efficient Layer Aggregation Networks (E-ELAN) to maximize gradient propagation and compound model scaling. The E-ELAN module can be interpreted as a recursive aggregation function $f: \mathbb{R}^n \rightarrow \mathbb{R}^n$ that optimizes feature reuse as in equation eq.8.

$$f_{E-ELAN}\ (x) = \emptyset_3(\emptyset_2(\emptyset_1(x)\oplus x)\ ) \qquad Eq.8$$

Here, $\emptyset_i$ denotes convolutional transformations and $\oplus$ stands for feature concatenation [22]. YOLOv7's anchor-free prediction head maps bounding boxes as point-based regression targets as equation eq.9.

$$t_x = \frac{x-x0}{w}, t_y = \frac{y-y0}{h}, t_w = log\left(\frac{w}{w0}\right), t_h = \log\left(\frac{h}{h0}\right) \qquad Eq.9$$

2.2 *YOLOv7 Architecture*

The traditional YOLOv7 based model includes convolutional layers with advanced blocks that is EELAN for improved gradient propagation and efficient learning. The following sections explain the basic YOLO v7 object detection steps.

Step 1: Data preprocessing

Initially the input image is preprocessed to ensure that the image is in a proper format and size.

Step 2: Backbone (Image Feature Extraction)

The backbone is the core of YOLOv7, it helps in extracting important image features. It introduces the EELAN to extract deep features. The feature extraction is performed by convolution operation using equation eq.10.

$$Y = \sigma(W * X) \qquad \text{Eq. 10}$$

Where X is the input feature map, W is the convolution kernal and W*X is calculated as equation eq.11.

$$Y_{i,j,k} = \sum_{a=0}^{A-1} \sum_{b=0}^{B-1} x_{i+a,j+b} * W_{a,b,k} + bis_k \qquad \text{Eq. 11}$$

Where, $Y_{i,j,k}$ = feature maps output at (i,j) and k channel; $x =$ input feature maps; w = image kernal; $bis_k =$ Kth channel position bias; $A * B =$ Kernal size.

Step 3: Neck (Feature Fusion)

The neck layers integrate multi-scale features to improve object detection with different sizes efficiently. Spatial Pyramid Pooling is used to enhance the receptive fields by using equation eq.12.

$$y = Concate\left(Maxpool_k(x), Maxpool_{k/2}(x), Maxpool_{k/4}(x)\right) \qquad \text{Eq. 12}$$

Step 4: Head (Bounding Box Prediction)

The detection head layer is held responsible for license plate bounding box using equation eq. 13, to calculate the abjectness score using equation eq.14 and calculate the class probability using equation eq.15. The final bounding box detection is done using equation eq.16

$$\hat{x} = \sigma(t_x) + C_x, \hat{y} = \sigma(t_y) + C_y \qquad \text{Eq.13}$$

$$P_{obj} = \sigma(t_{obj}) \qquad \text{Eq.14}$$

$$p_{cls} = \frac{e^{ti}}{\sum_{j-1}^{C} e^{tj}} \qquad \text{Eq.15}$$

$$Detected = [\hat{x}, \hat{y}, \widehat{w}, \hat{h}, P_{obj}, P_{cls}] \qquad \text{Eq.16}$$

3. Proposed Method

This section presents the mathematical derivation of the proposed skewed license plate detection method based on theta-angle computation.

3.1 *Contrast Enhancement using CLAHE*

To handle poor visibility and enhance license plate features in complex weather or low-light images, Contrast Limited Adaptive Histogram Equalization

(CLAHE) is applied on the L-channel of the LAB color space. Initially convert the input RGB image I(x,y) to LAB using equation eq.17. And apply CLAHE to the luminance channel L using equation eq.18.

$$I_{LAB} = CVT^{COLOR}(I, RGB \rightarrow LAB) \qquad Eq.17$$

$$L_{eq} = CLAHE(L), CLAHE(L) = \frac{L-L_{min}}{L_{max}-L_{min}} .255 \qquad Eq.18$$

3.2 *Contour Detection and Aspect Ratio Filtering*

To locate the potential license plate regions, the image is thresholded and contours are extracted using the following steps:

- Convert to grayscale using equation eq.19.

$$I_{gray} = 0.299.R + 0.587.G + 0.114.B \qquad Eq.19$$

- Apply adaptive thresholding using equation eq.20

$$I_{bin} = AdaptiveThresh\left(I_{gray}\right) \qquad Eq.20$$

- Apply morphological operations using equation eq.21

$$I_{morph} = Dilate\left(Erode(I_{bin})\right) \qquad Eq.21$$

- Detect the contours C={ci}using equation eq.22, and compute aspect ratio using equation eq.23

$$\text{Contour area } A = w.h \qquad Eq.22$$

$$\text{Aspect ratio AR} = \frac{w}{h} \qquad Eq.23$$

- Apply filtering using equation eq.24

$$A > A_{thresh}, 2 \leq AR \leq 5 \qquad Eq.24$$

3.3 *Perspective Correction Using Homography*

For license plates with skewed quadrilateral shapes, homography transformation is applied to project the region into a canonical rectangular frame. Let the detected plate corners be P={p1,p2,p3,p4} and the target rectangle points be Q={q1,q2,q3,q4}. Then a homography matrix H is computed using equation eq.25. Here $H \in \mathbb{R}^{3*3}$ satisfies:

$$\begin{bmatrix} u \\ v \\ 1 \end{bmatrix} \sim H \begin{bmatrix} x \\ y \\ 1 \end{bmatrix}, q_i \sim H.P_i \qquad Eq.25$$

3.4 *Rotation Correction Using Affine Transformation*

To correct tilted license plates that are not horizontally aligned, estimate the theta angle of skew and apply an affine rotation. From top-left and top-right corner points using equation eq.26 and compute the tilt theta angle using equation eq.27

$$P1=(a1,b1), P2=(a2,b2) \qquad Eq.26$$

$$\theta = \arctan\left(\frac{b_2 - b_1}{a_2 - a_1}\right) \qquad Eq.27$$

Construct the rotation matrix as equation eq.28 and apply affine transformation around the center c using equation eq.29. Figure 1 lists the different theta angle calculated along with the tilt directions.

$$R(-\theta) = \begin{bmatrix} cos\theta \ Sin\theta \\ -Sin\theta \ Cos\theta \end{bmatrix} \qquad Eq.28$$

$$X` = R(-\theta)(x - c) + c \qquad Eq.29$$

This ensures horizontal alignment for OCR and detection.

Image Name	Tilt Angle (degrees)	Tilt Direction
46.jpg	0	Horizontal
58.jpg	0	Horizontal
111.JPG	17.57	Clockwise
123.JPG	12.57	Clockwise
126.JPG	4.52	Clockwise
134.JPG	6.11	Clockwise
138.JPG	1.47	Clockwise
145.JPG	16.7	Clockwise
147.JPG	5.28	Clockwise
149.JPG	16.76	Clockwise
152.JPG	26.04	Clockwise
158.JPG	16.13	Clockwise
16.jpg	0.76	Clockwise
17.jpg	1.52	Clockwise
173.JPG	13.92	Clockwise

Figure 1
Theta angle and tilt direction results

4. Results and Discussion

The evaluation of license plate detection task is crucial to ensure the accuracy and reliability of the proposed model. Mean Average Precision (mAP) is frequently used by performance metrics to evaluate the license plate detection models. The task of license plate detection involves identifying the license plate from the whole vehicle images and classifying whether it is correctly detected or not. The proposed model is evaluated using precision, recall, accuracy and ROC curve i.e. Receiver Operating Characteristic. Precision measures how often the model predicts the correct license plate. High value of precision shows less False Positive values i.e. minimal error rate. The precision is calculated using the equation eq.30. Similar things are discussed in [20], [21], [22]

$$\text{Precision} = TP/(TP + FP) \qquad \text{Eq. 30}$$

Recall is represented as a measure of quality; it measures the model's ability to detect all the relevant objects. The recall is calculated using the equation eq.31

$$\text{Recall} = TP/(TP + FN) \qquad \text{Eq.31}$$

Where:

- **TP**: True Positives (correctly predicted license plates)
- **FP**: False Positives (incorrectly predicted objects as license plates)
- **FN**: False Negatives (missed license plates)

Mean Average Precision (mAP) is the average of precision-recall curves over the multiple IoU threshold. mAP is calculated using equation eq.32 and eq. 33.

$$\text{mAP} = \frac{1}{C}\sum_{c=1}^{C} AP_C \qquad \text{Eq.32}$$

$$\text{AP} = \sum_{i=1}^{n}(Rec_i - Rec_{i-1})P_i \qquad \text{Eq.33}$$

Here, $P_i = precision\ at\ recall\ Rec_i$

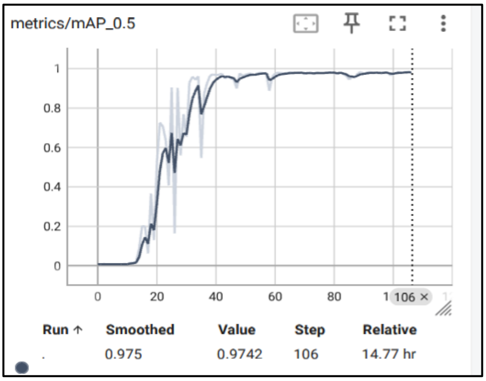

Figure 2
mAP_0.5 for license plate detection

ROC curve represents the True Positive rate against the False Positive rate. The quantitative evaluation showcase that derived mathematical model achieves the highest accuracy in detecting vehicle license plates including the tilted plate detection. The proposed model achieved 99% accuracy for correctly identifying license plates, with a negligible 1% False Negative rate. The clear distinction between the predicted and actual values confirms the model's robust performance with minimal errors. The mAP curve shows that the model achieved a stable and high performance with a final mAP value of 0.9742 at step 106, indicating excellent detection capabilities. The curve in figure 2 illustrates a sharp increase during the early stages of training, followed by a stable plateau, confirming the model's convergence. The ROC curve for the proposed detection model achieved an AUC of 0.98, significantly outperforming the baseline model with an AUC of 0.85. The higher AUC score demonstrates the improved trade-off between the True Positive rate (TPR) and False Positive rate (FPR), proving superior discrimination capability in identifying license plates under challenging conditions.

5. Conclusion and Future Work

The proposed geometrically enhanced skew detection model effectively addresses challenges in detecting tilted and skewed license plates under complex conditions. By estimating the orientation angle (theta) and applying rotation and homography transformations, the model improves spatial alignment and detection accuracy. Tested on 1100 diverse images, it achieved 99% accuracy and improved AUC from 0.85 to 0.98, outperforming traditional detection model. These results confirm the benefit of angular correction and normalization. Future work will focus on enhancing the detection of moving vehicles, addressing challenges associated with motion blurry and rapid movement. This includes the integration of adaptive angle estimation techniques using trigonometric optimization, refinement of the homography transformation through dynamic control point selection, and incorporation of probabilistic models to better handle uncertainty in plate orientation.

References

[1] H. Li, P. Wang, and C. Shen, "Toward End-to-End Car License Plate Detection and Recognition with Deep Neural Networks," *IEEE Transactions on Intelligent Transportation Systems*, vol. 20, no. 3, pp. 1126–1136 (Aug. 2019), doi: 10.1109/TITS.2018.2847291.

[2] N. N. Kamal and E. Tariq, "License Plate Tilt Correction: A Review," *Engineering and Technology Journal,* vol. 39, no. 1B, pp. 1–8 (2021).

[3] K. Deb, I. Khan, A. Saha, and K.-H. Jo, "An Efficient Method of Vehicle License Plate Recognition Based on Sliding Concentric Windows and Artificial Neural Network," *Procedia Technology,* vol. 4, pp. 812–819 (2012).

[4] P. Jiang, D. Ergu, F. Liu, Y. Cai, and B. Ma, "A review of YOLO algorithm developments," *Procedia Computer Science,* vol. 199, pp. 1066–1073 (2022).

[5] M. Hussain, "YOLO-v1 to YOLO-v8, the Rise of YOLO and Its Complementary Nature Toward Digital Manufacturing and Industrial Defect Detection," *Machines*, vol. 11, no. 7, pp. 677 (2023).

[6] J. Terven, D.-M. Córdova-Esparza, and J.-A. Romero-González, "A Comprehensive Review of YOLO Architectures in Computer Vision: From YOLOv1 to YOLOv8 and YOLO-NAS," *Machine Learning and Knowledge Extraction*, vol. 5, no. 4, pp. 1680–1716 (2023).

[7] S. Parvin, L. J. Rozario, and M. E. Islam, "Vehicle Number Plate Detection and Recognition Techniques: A Review," *Advances in Science, Technology and Engineering Systems Journal*, vol. 6, no. 2, pp. 423–438 (Mar. 2021), doi: 10.25046/aj060249.

[8] N. Shidore and M. Patwardhan, "Automatic Vehicle Number Plate Recognition System Using Optical Character Recognition and Artificial Neural Network," *International Journal of Computer Applications*, vol. 1, no. 21, pp. 28–32 (2010).

[9] P. I. Reji and V. S. Dharun, "License Plate Localization: A Review," *International Journal of Engineering Trends and Technology* (IJETT), vol. 10, no. 13, pp. 604–615 (Apr. 2014).

[10] S. A. Pagore and M. S. Deshpande, "Car License Plate Detection," *International Journal of Computer Applications*, vol. 128, no. 13, pp. 8–11 (Oct. 2015), doi: 10.5120/ijca2015906716.

[11] X. Zhang, N. Gu, H. Ye, and C. Lin, "Vehicle License Plate Detection and Recognition Using Deep Neural Networks and Generative Adversarial Networks," *Journal of Electronic Imaging*, vol. 27, no. 4, pp. 043056 (Aug. 2018), doi: 10.1117/1.JEI.27.4.043056.

[12] Slimani, A. Zaarane, W. Al Okaishi, I. Atouf, and A. Hamdoun, "An automated license plate detection and recognition system based on wavelet decomposition and CNN," *Array*, vol. 8, pp. 100040 (2020).

[13] J. Redmon, S. Divvala, R. Girshick, and A. Farhadi, "You Only Look Once: Unified, Real-Time Object Detection," in Proc. IEEE Conf. Comput. Vis. Pattern Recognit. (CVPR), pp. 779– 788 (2016).

[14] J. Redmon and A. Farhadi, "YOLO9000: Better, Faster, Stronger," in Proc. IEEE Conf. Comput. Vis. Pattern Recognit. (CVPR), pp. 7263–7271 (2017).

[15] J. Redmon and A. Farhadi, "YOLOv3: An Incremental Improvement," arXiv preprint arXiv:1804.02767 (2018).

[16] A. Bochkovskiy, C.-Y. Wang, and H.-Y. M. Liao, "YOLOv4: Optimal Speed and Accuracy of Object Detection," arXiv preprint arXiv:2004.10934 (2020).

[17] D. Thuan, Evolution of YOLO Algorithm and YOLOv5: The State-of-the-Art Object Detection Algorithm, Bachelor's thesis, Oulu University of Applied Sciences, Oulu, Finland (2021).

[18] C. Gupta, N. S. Gill, P. Gulia, and J. M. Chatterjee, "A Novel Fine-tuned YOLOv6 Transfer Learning Model for Real-Time Object Detection," *Journal of Real-Time Image Processing*, vol. 20, article no. 42 (Apr. 2023), doi: 10.1007/s11554-023-01299-3.

[19] B. Sun, K. Bi, and Q. Wang, "YOLOv7-FIRE: A Tiny-Fire Identification and Detection Method Applied on UAV," AIMS Mathematics, vol. 9, no. 5, pp. 10775–10801 (Mar. 2024), doi: 10.3934/math.2024526.

[20] H. Harjule, P. Priyanka, V. Tiwari, and A. Kumar, "Mathematical models to predict COVID-19 outbreak: An interim review," *Journal of Interdisciplinary Mathematics*, vol. 24, no. 2, pp. 259–284 (2021).

[21] C. Meshram, "Modified ID-based public key cryptosystem using double discrete logarithm problem," *International Journal of Advanced Computer Science and Applications* (IJACSA), vol. 1, no. 6 (2010).

[22] M. Orouskhani, Y. Orouskhani, M. Mansouri, and M. Teshnehlab, "A novel cat swarm optimization algorithm for unconstrained optimization problems," *International Journal of Information Technology and Computer Science*, vol. 5, no. 11, pp. 32–41 (2013).

Received April, 2025